Effects of crossed flux on magnetization dynamics and magnetic relaxation of melt-textured $Y_1Ba_2Cu_3O_{7-x}$

1996 J. Phys.: Condens. Matter 8 8339

(http://iopscience.iop.org/0953-8984/8/43/025)

J. Phys.: Condens. Matter **8** (1996) 8339–8350. Printed in the UK

Effects of crossed flux on magnetization dynamics and magnetic relaxation of melt-textured $Y_1Ba_2Cu_3O_{7-x}$

Sadia Manzoor and S K Hasanain

Department of Physics, Quaid-i-Azam University, Islamabad 45320, Pakistan

Received 12 March 1996, in final form 28 May 1996

Abstract. We report magnetization measurements of melt-textured $Y_1Ba_2Cu_3O_{7-x}$ in a crossed-flux configuration (CFC), i.e. in the presence of two mutually perpendicular flux components. We have measured the $M(H)$ loops of the *a–b* planes and their dependence on the field sweep rate in the presence of various remnant fluxes along the *c* axis. Furthermore, we have carried out magnetic relaxation studies of the *a–b* plane moment in the CFC, and compared the results with those obtained in the single-flux configuration (SFC), i.e. when there is no *c*-axis remanence. Our results in three different experiments show enhanced flux entry along the *a–b* planes in the CFC. We interpret this in terms of a suppression of the shielding currents and discuss flux cutting as a possible mechanism which can lead to it.

1. Introduction

Recently interest has revived in the vortex dynamics of high-T_c superconductors in the crossed-flux configuration (CFC). By this we mean the simultaneous presence of two non-parallel families of flux lines, which in most cases are taken to be mutually orthogonal. Such situations had been discussed [1] in the context of the low-T_c materials for the analysis of the force-free configuration ($\boldsymbol{J}_{\parallel} \times \boldsymbol{B} = \boldsymbol{0}$), where $\boldsymbol{J}_{\parallel}$ is the component of the current parallel to the magnetic induction $\boldsymbol{B}$. In a CFC the current shielding one flux component is, over part of its path, parallel to the other component of flux. If $\boldsymbol{J}_{\parallel}$ is larger than a critical value $\boldsymbol{J}_{C\parallel}$, flux-cutting events can occur, leading to a breakdown of the force-free configuration [1–3]. The concept of flux cutting and reconnection leading to dissipative processes in such configurations had been invoked. An associated discussion has had to do with the effect of the transverse flux density on the critical state currents of the longitudinal flux [1]. More recently this debate has focused on the possibility of flux cutting in the high-T_c materials, and the effects of anisotropy and flux line curving on the flux-cutting barriers [4, 5]. These ideas have obvious implications for the stability of an entangled glass or liquid of flux lines. The CFC is not purely of academic interest but is also important to understand because, in many magnetomechanical applications of superconductors, similar situations may be encountered. That is, there is an applied field and there are parasitic or remnant fields in some other direction, which affect the overall response.

There exists considerable controversy regarding the role of transverse flux on the motion of flux in a longitudinal direction. Magnetic studies by Park and co-workers [6, 7] on $YBa_2Cu_3O_{7-x}$ (YBCO) single crystals [6, 7] show that a strongly pinned remanence along the *c* axis inhibits flux entry along the *a–b* planes. These results are in direct contrast with those obtained by LeBlanc and co-workers [8, 9] on sintered tubes of (YBCO) material,

0953-8984/96/438339+12$19.50

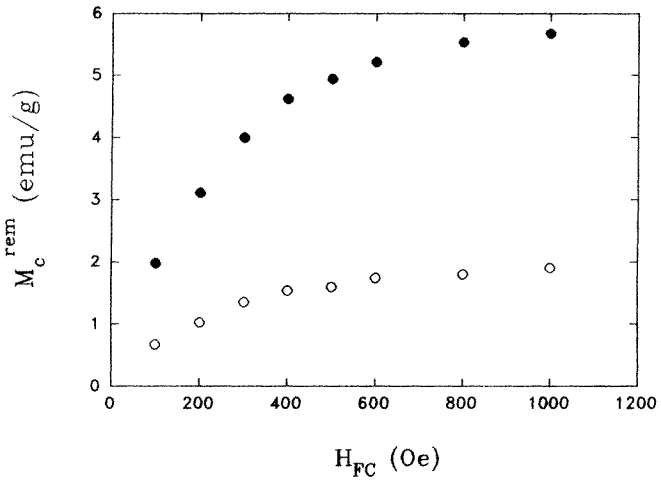

Figure 1. Remnant moment M_c^{rem} along the c axis (●) and the remnant moment M_{ab}^{rem} along the a–b planes (○) against cooling field H_{FC}.

and by us [10] on melt textured samples of YBCO. LeBlanc and co-workers showed that flux-cutting events take place in a CFC, and the presence of a toroidal field suppressed the shielding currents for the axial field. Our studies also showed that the presence of a transverse flux along the c axis actually enhances flux entry in a longitudinal direction (i.e. along the a–b planes), by suppressing the shielding currents associated with the a–b plane moment. This apparent discrepancy will be discussed in detail in the conclusions.

Recent magneto-optical investigations by Indenbom *et al* [11] show that, in a strongly correlated 3D system, the force-free configuration of current and vortices can be very stable, and a perpendicular field component does not penetrate through an array of longitudinal flux lines. In a weakly coupled 2D system such as BSCCO on the other hand, the transverse flux does not appear to influence the motion of the longitudinal flux lines. As pointed out in [11], a breakdown of the force-free configuration can occur in vortex systems with weak internal connections, such as 2D systems, or even in anisotropic 3D superconductors in which the transverse flux can penetrate from the ends, where the force-free configuration is locally not realized. In such a situation, vortex lattice cutting and reconnection appear to be an important mechanism, particularly when large intervortex angles can be established, since cutting barriers are minimal for mutually perpendicular flux lines [4].

In a previous experiment we measured the magnetization M_{ab} of melt-textured samples along the a–b planes, in the presence of a field-cooled remnant flux along the c axis [10]. We clearly observed a decreased diamagnetic signal for M_{ab} as the magnitude of the remnant flux along the c axis was increased. Since the ease of flux entry in such a measurement can be related to a decrease in the effective activation barriers for flux movement, we have performed experiments which can give more quantitative results on the decrease in the activation barriers with increasing transverse flux density. In the present paper, we extend our previous investigations to include magnetic relaxation studies of the a–b plane moment in the presence of a remnant flux along the c axis and obtain the relaxation rate $S = (1/M_0)[\partial M/\partial(\ln t)]$.

Additionally we have investigated the effects of various field sweep rates on the $M(H)$ loops in the CFC, and compared the results with the single-flux case, i.e. in the absence

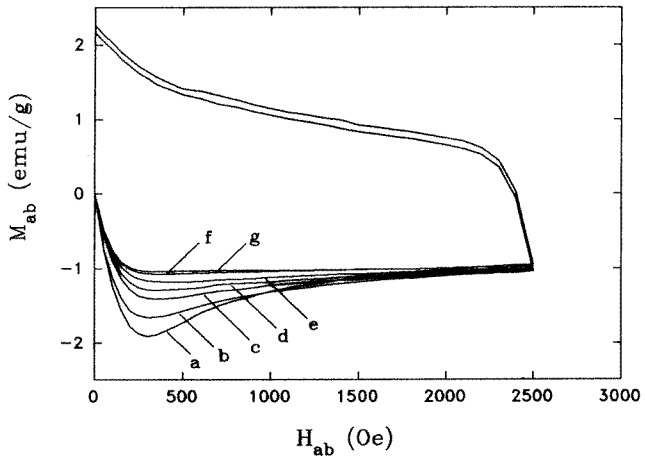

Figure 2. $M(H)$ loops of the a–b plane for the single-flux case (curve a), as well as for different cooling fields parallel to the c axis: curve b, $H_{FC} = 100$ Oe; curve c, $H_{FC} = 200$ Oe; curve d, $H_{FC} = 300$ Oe; curve e, $H_{FC} = 400$ Oe; curve f, $H_{FC} = 500$ Oe; curve g, $H_{FC} = 600$ Oe. The loop for $H_{FC} = 800$ Oe has been measured but is not shown in the figure for clarity. The outer curve for the field-decreasing branch corresponds to the single-flux loop (curve a), while the inner curve corresponds to $H_{FC} = 600$ Oe (curve g). The other curves on the field decreasing branch lie between these two but are not shown for clarity.

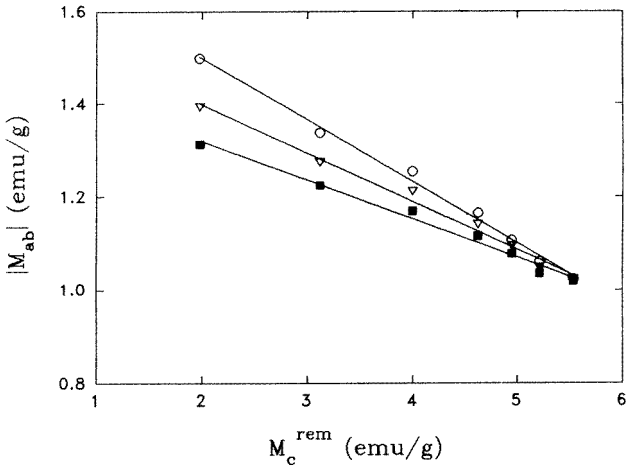

Figure 3. Magnitude of the diamagnetic response $|M_{ab}|$ of the a–b planes as a function of the remanence M_c^{rem} along the c axis. $|M_{ab}|$ has been extracted from figure 2 at three values of the a–b-plane field: ○, $H_{ab} = 600$ Oe; ▽, $H_{ab} = 800$ Oe; ■, $H_{ab} = 1000$ Oe. The straight lines serve as a guide to the eye.

of a c-axis remanence. These experiments yield valuable information on the dynamics of vortex motion in the CFC and have been used to extract the so-called sweep creep rate $C = (1/M)[\partial M/\partial(\ln \dot{H})]$, as well as the $E(J)$ behaviour in the crossed-flux mode for various remnant flux densities.

2. Experiments

The experimental technique and details of sample preparation and characterization have been discussed in [10]. Here we outline the main points of the experimental procedure. The specimen used is a melt-textured $YBa_2Cu_3O_{7-x}$ sample (3 mm × 3 mm × 3 mm). It has an anisotropy ratio $\Gamma = (M_c^{rem})_s/(M_{ab}^{rem})_S \approx 3$. Here, $(M_c^{rem})_S$ and $(M_{ab}^{rem})_s$ are the saturation values of the remnant magnetizations obtained by field-cooling along the c axis and the a–b planes, respectively, at $T = 77$ K (figure 1). The measurements have been made on a commercial vibrating-sample magnetometer (VSM), in which the magnetic field is applied along the x direction. The CFC is prepared as follows. The sample is field cooled along the c axis and, after reducing H to zero, the remnant flux M_c^{rem} obtained. The cooling field H_{FC} has been varied between 0 and 1000 Oe. The variation in M_c^{rem} with cooling field H_{FC} is shown in figure 1. After H_{FC} is turned off and the remnant flux parallel to the c axis obtained, the sample is rotated through 90°, such that the a–b plane now lies along the x direction. It has been checked that the c-axis remanence rotates rigidly and does not give a projection on the VSM pick-up coils lying along the x direction. Following the rotation of M_c^{rem}, a magnetic field is applied along the a–b planes, and the magnetization $M_{ab}(H_{ab})$ is measured. In the magnetic relaxation experiments, the a–b-plane field is ramped up to 600 Oe at the rate of 5 Oe s^{-1}, and the relaxation data are taken at this value of H_{ab}. In the $M(H, \dot{H})$ experiments, H_{ab} is swept around a half-loop ($0 \rightarrow H_{max} \rightarrow 0$), the maximum field being 2500 Oe. These latter experiments have been performed at five different sweep rates varying between 8 and 187 Oe s^{-1}. All studies have been carried out at 77 K.

3. Results and discussion

3.1. M(H) loops in the crossed-flux configuration

The *in-situ* measurements of the a–b-plane moment M_{ab} and the c-axis remanence M_c^{rem} have been described and discussed in detail in [10]. Here we show in figure 2 only the variation in M_{ab} versus H_{ab} for various magnitudes of M_c^{rem}, as well as the single-flux loop of the a–b planes (i.e. with $M_c^{rem} = 0$). (These loops were measured at a field sweep rate of 17 Oe s^{-1}.) We note that, as M_c^{rem} is increased, the response of the a–b planes becomes less diamagnetic. This indicates that, in the presence of a c-axis remanence, a large amount of flux enters along the a–b planes. The loops become increasingly flatter as M_c^{rem} is increased and seem to merge at some field larger than 2500 Oe. There exist finite differences between the virgin loop and the crossed-flux loops even at $H_{ab} = 2500$ Oe. These differences persist on field reversal, indicating that the transverse flux has not been completely expelled. In [10] we showed that this enhanced entry of the a–b-plane flux is accompanied by a steady decrease in the c-axis remanence, which we argued was due to its expulsion following cutting. It has been shown in [10] that the differences between the $M_{ab}(H)$ loops in the crossed and uncrossed configurations could not be explained away by assuming a rotation of the c-axis flux towards the a–b planes. At low fields ($H_{ab} \leqslant 200$ Oe), the changes in M_c^{rem} with field were too small to account for the difference between the a–b-plane magnetizations in the crossed and uncrossed modes. At higher fields, however, the change in M_c^{rem} increases steadily, while the differences between the a–b-plane loops in the crossed and uncrossed modes diminish towards zero. M_c^{rem} does not appear to rotate towards the a–b planes, as this would be reflected in persisting differences between the uncrossed- and crossed-flux loops. This leads one to believe that the c-axis flux is being expelled as the a–b-plane field increases to large values.

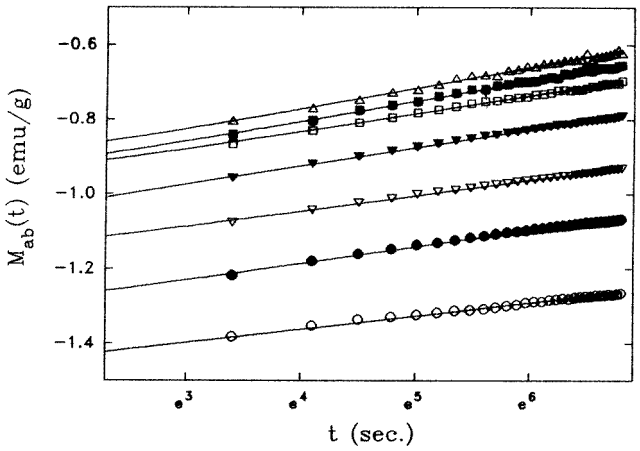

Figure 4. Magnetization relaxation data taken after a field ramp to $H_{ab} = 600$ Oe for the SFC (○), as well as for the CFC with $H_{FC} = 100$ Oe (●), $H_{FC} = 200$ Oe (▽), $H_{FC} = 400$ Oe (▼), $H_{FC} = 600$ Oe (□), $H_{FC} = 800$ Oe (■) and $H_{FC} = 1000$ Oe (△). The straight lines are fits to equation (1).

From figure 2 the values of M_{ab} have been extracted at $H_{ab} = 600$, 800 and 1000 Oe. In figure 3 these have been plotted as a function of M_c^{rem}, the c-axis remanence at the start of the hysteresis loop. We do not use the width ΔM_{ab} of the hysteresis loop for our analysis, rather only the value of $|M_{ab}|$ on the ascending field branch. This choice is motivated by the fact that the crossed flux leaves its signature primarily on the magnetization in the ascending field branch. In figure 3 we find that, for all three values of H_{ab}, M_{ab} decreases linearly with increasing M_c^{rem}, its rate of change (with M_c^{rem}) being smaller for higher values of H_{ab}. The convergence of the lines is reflective of the flatness of the $M(H)$ loops for large remanences. According to the critical state model, M_{ab} is a measure of the appropriate shielding currents. Thus figure 3 indicates a continuous linear decrease in the shielding currents as the transverse remnant flux is increased.

3.2. Magnetic relaxation studies in the crossed-flux configuration

Although there exist extensive data on relaxation in the single-flux configuration (SFC) (both parallel and perpendicular to the c axis) [12–14], we have not come across studies of relaxation effects in a CFC. The relaxation or creep process is understood to take place over current-dependent activation energy barriers $U_{eff}(J)$ [15, 16]. A suppression of the critical currents in the presence of crossed flux (as can be seen from figure 3) would obviously affect the height of these activation energy barriers. The detailed dependence would vary with the particular $U_{eff}(J)$ relationship which is valid in the temperature and field regimes under consideration.

We have measured the temporal decay of the a–b-plane moment in a short time window of 900 s with a sampling time of 1 s, following a field ramp of 600 Oe at the rate of about 5 Oe s^{-1}. Figure 4 shows the $M_{ab}(t)$ curves for the single-flux case ($M_c^{rem} = 0$), as well as for six values of the crossed flux. (The closeness of the curves at high remanences is again only an artefact of the saturation of M_c^{rem} with H_{FC}.) We find a logarithmic time

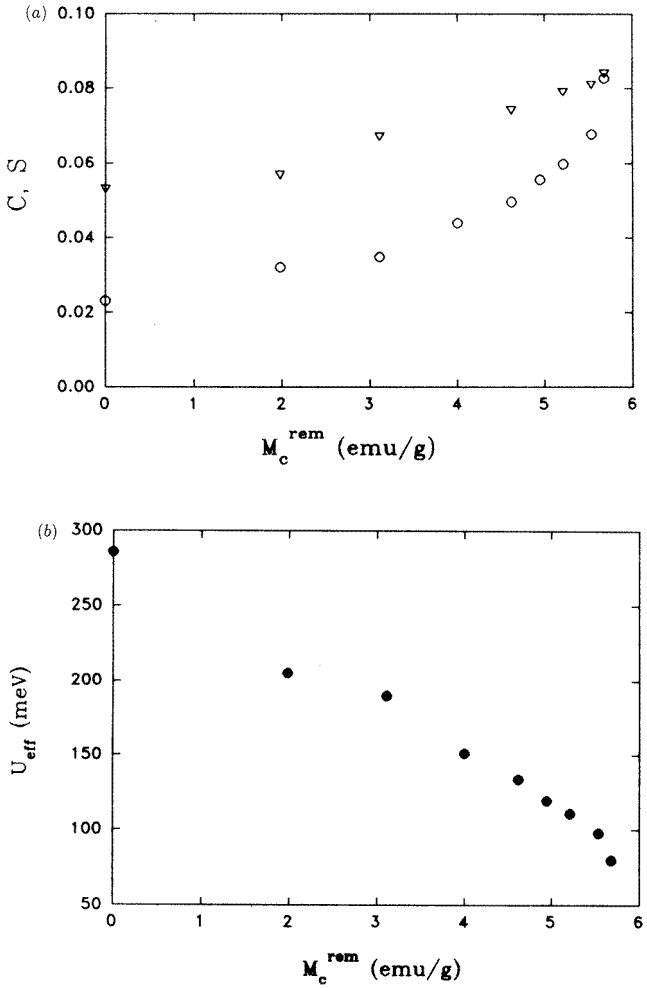

Figure 5. (*a*) Dependences of the relaxation rate S (○), and sweep creep rate C (▽) on M_c^{rem}. The values of C and S have been obtained for $H_{ab} = 600$ Oe. (*b*) Effective activation energy U_{eff} for the motion of the *a*–*b*-plane flux as a function of M_c^{rem}. U_{eff} has been obtained from the values of S according to $S = kT/U_{eff}$.

dependence of the *a*–*b*-plane magnetization, with the data fitting the expression

$$M(t) = M_0[1 + S\ln(1 + t/\tau)]. \tag{1}$$

well. Here S is the normalized relaxation rate and τ is some macroscopic relaxation time. For relatively small time windows the collective creep model can be approximated to give a logarithmic time dependence for $M(t)$ [17]. In this approximation, the rate $S = (1/M_0)[\partial M/\partial(\ln t)]$ yields the activation barrier $S = kT/U_{eff}(J)$. Typical forms for $U_{eff}(J)$ are the classical linear (Anderson) form $U_{eff}(J) = U_0[1 - (J/J_c)]$, and the non-linear dependence $U_{eff}(J) \sim U_0(J_c/J)^{\mu}$. With increasing field, one usually obtains a decrease in $U_{eff}(J)$, reflecting the decreased value of the critical current J_c.

We find that the presence of crossed flux does not change the functional form of the $M(t)$ dependence at least in the short time window. Its only effect seems to lie in an

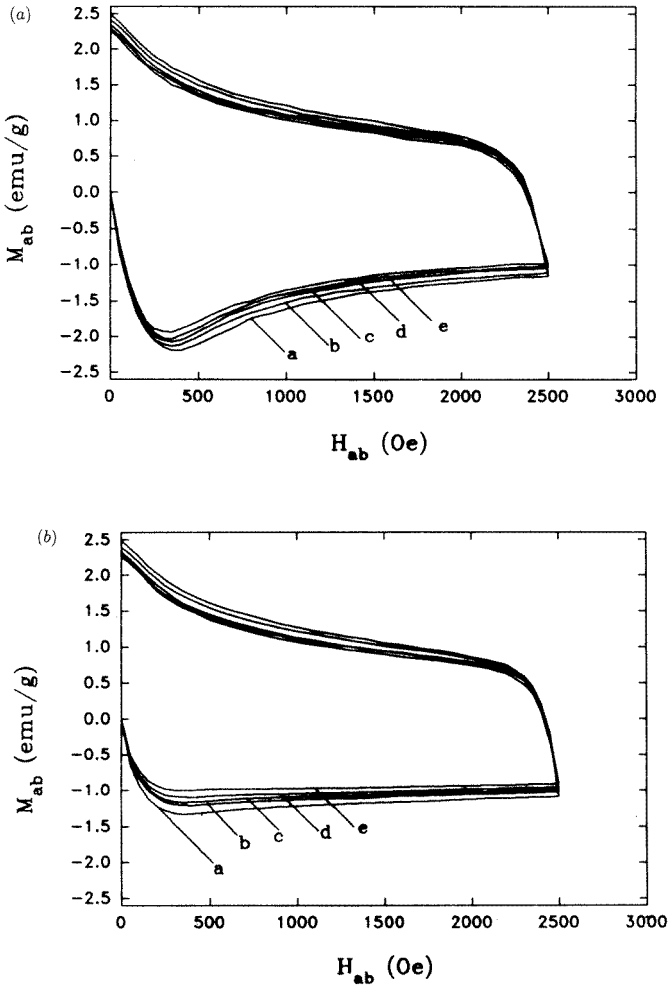

Figure 6. (*a*) $M_{ab}(H_{ab}, \dot{H}_{ab})$ loops for the single-flux configuration with $\dot{H}_{ab} = 187$ Oe s^{-1} (curve a), 92 Oe s^{-1} (curve b), 33 Oe s^{-1} (curve c), 17 Oe s^{-1} (curve d) and 8 Oe s^{-1} (curve e). (*b*) $M_{ab}(H_{ab}, \dot{H}_{ab})$ loops measured in the crossed-flux configuration with $H_{FC} = 800$ Oe and $\dot{H}_{ab} = 187$ Oe s^{-1} (curve a), 92 Oe s^{-1} (curve b), 33 Oe s^{-1} (curve c), 17 Oe s^{-1} (curve d) and 8 Oe s^{-1} (curve e).

enhancement of the relaxation rate, from $S = 0.023$ in the single-flux mode to $S = 0.083$ in the presence of a transverse remanence of 5.7 emu g^{-1} (corresponding to a cooling field of 1000 Oe). This corresponds to a decrease in U_{eff} from 280 to 80 meV. It is physically more relevant to represent S and U_{eff} as functions of the flux trapped along the c axis (figure 5). Here we can see that the variation in U_{eff} with M_c^{rem} is reasonably linear and is reminiscent of the linear behaviour of $M_{ab}(\propto J)$ with M_c^{rem}. The relaxation rate on the other hand increases very strongly with increasing M_c^{rem} at higher values of the remnant flux. The relaxation data have been taken at $H_{ab} = 600$ Oe, a field at which there is a significant amount of c-axis flux present in the sample, as can be seen from the differences between the single-flux loop and the crossed-flux loops in figure 2.

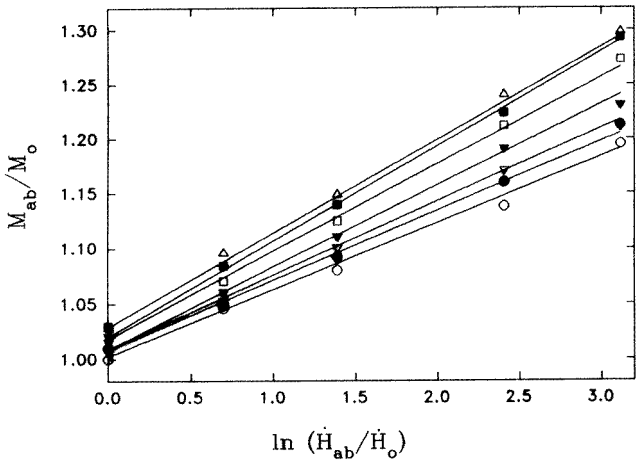

Figure 7. Normalized magnetization versus logarithm of the normalized sweep rate at $H_{ab} =$ 600 Oe and different cooling fields, where M_0 has been defined in the text and $\dot{H}_0 = 8$ Oe s^{-1}, the slowest sweep rate used: ○, single-flux data; ●, $H_{FC} = 100$ Oe; ▽, $H_{FC} = 200$ Oe; ▼, $H_{FC} = 400$ Oe; □, $H_{FC} = 600$ Oe; ■, $H_{FC} = 800$ Oe; △, $H_{FC} = 1000$ Oe. The straight lines are fits to equation (2).

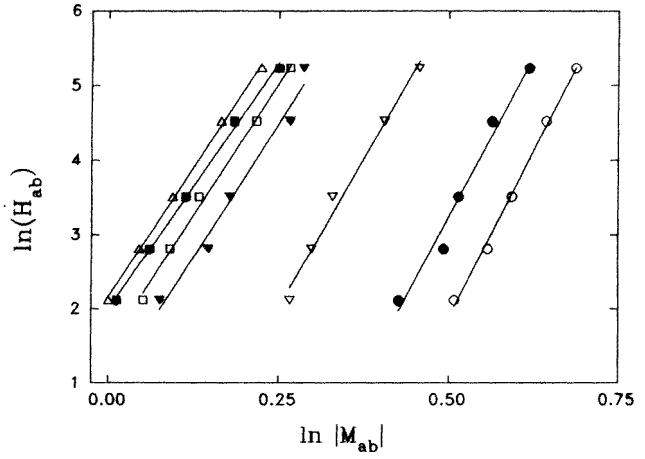

Figure 8. The log–log plot of sweep rate $\dot{H}_{ab}$ and magnetization $|M_{ab}|$ at $H_{ab} = 600$ Oe for different cooling fields. Data are shown for the single-flux case (○), $H_{FC} = 100$ Oe (●), $H_{FC} = 200$ Oe (▽), $H_{FC} = 400$ Oe (▼), $H_{FC} = 600$ Oe (□), $H_{FC} = 800$ Oe (■) and $H_{FC} = 1000$ Oe (△). The straight lines are fits to a linear equation of the form $\ln \dot{H}_{ab} = n \ln |M_{ab}| + C$ where C is a constant and n the slope of the lines. n is thus the exponent of the power law $\dot{H}_{ab} = A|M_{ab}|^n$.

At a cooling field of 1000 Oe, S increases by about 300% of its value in the single-flux mode. The very rapid increase in S (and related decrease in U_{eff}) due to the crossed flux motivates the obvious question as to the mechanism whereby the transverse flux facilitates the entry of the longitudinal flux. The most plausible explanation seems to be that the transverse flux enables the longitudinal flux to cut through and then to rejoin within the

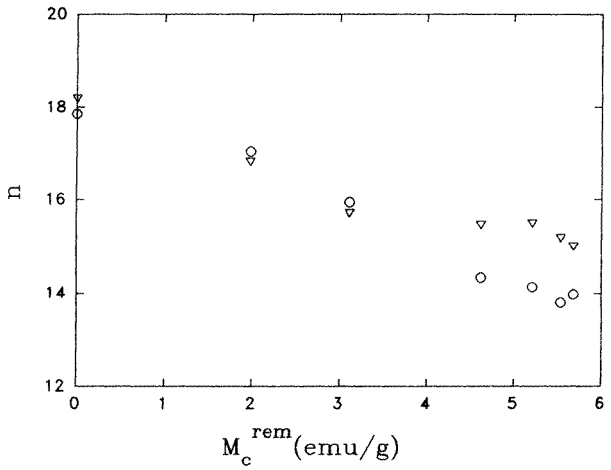

Figure 9. Variation in the exponent n obtained from figure 8 as a function of the c-axis remanence for two different values of the a–b-plane field: ○, $H_{ab} = 600$ Oe; ▽, $H_{ab} = 1000$ Oe.

sample. The angle ($\theta = \pi/2$) which nominally exists between the two flux families, and the relatively low degree of correlation or coherence of the lines also help to realize the process of cutting. While the former ensures that repulsive effects between vortex cores are minimized, the latter, as discussed in [2], makes it possible for transverse vortex segments to curve and tilt without entailing large displacements of the vortex elements at extended distances.

3.3. Sweep rate dependence of magnetization in a crossed-flux configuration

The effect of field sweep rate on the magnetization of high-T_c superconductors has been well established [18–21]. Basically, the effect of ramping a magnetic field is to generate an electric field proportional to the sweep rate $\dot{H}$, which in turn generates currents according to the particular $E(J)$ dependence in that part of the phase space. The currents thus generated are manifested as additional magnetization.

Various models which invoke flux diffusion and drift dynamics have been proposed to explain this dependence of the magnetization on the sweep rate of the applied field. It has been shown that the width of the hysteresis loop increases with increasing sweep rate. M is found to be logarithmically dependent on $\dot{H}$:

$$M = M_0(H, T)[1 + C \ln(\dot{H}/\dot{H}_0)] \tag{2}$$

where $\dot{H}$ is the sweep rate of the applied field and M_0 is the magnetization associated with the rate $\dot{H}_0$.

To investigate the effect of the crossed flux on the above relationship and the E–J dependence, we have carried out experiments in the CFC at five different sweep rates from 8 to 187 Oe s^{-1}. Each set of five $M_{ab}(H_{ab}, \dot{H}_{ab})$ loops has been obtained for a given value of M_c^{rem}. There was a total of seven such sets measured, corresponding to cooling fields $H_{FC} = 0$, 100, 200, 400, 600, 800 and 1000 Oe. In figure 6(a), the broadening of the $M_{ab}(H_{ab})$ loops with increasing sweep rates in the SFC is evident. Figure 6(b) shows the $M_{ab}(H_{ab}, \dot{H}_{ab})$ loops in the CFC for a cooling field of 800 Oe, corresponding to a remnant flux of 5.5 emu g^{-1}.

We find that our $M_{ab}(H_{ab}, \dot{H}_{ab})$ data fit equation (2) well (figure 7), for all values of the cooling fields and $H_{ab} = 600$ Oe. The value of C has been obtained from these fits and is shown in figure 5(a) as a function of M_c^{rem}. Like the relaxation rate S, C too increases with increasing transverse flux. The magnitude of C, however, is generally larger than that of S, although the difference does seem to decrease towards higher values of M_c^{rem}. In this context it is important to realize that the relaxation and the sweep-creep ($M(H, \dot{H})$) experiments explore the E–J–B surface under different conditions. In the relaxation experiments, E and J change during the measurement whereas B is approximately constant while, in the sweep-creep experiments, the electric field is constant, being proportional to $\dot{H}$ [22].

Further evidence of reduced pinning in the CFC has been obtained from the variation in the E–J behaviour with various magnitudes of the crossed flux. In a sweep-creep experiment, as the magnetic field is swept around the loop, an electric field is induced, and the dependence of the loop width ΔM on $\dot{H}$ provides valuable further information. Caplin *et al* [22] show that this electric field is directly proportional to the applied sweep rate. Taking $\Delta M_{ab} \propto J$, the $M_{ab}(H_{ab}, \dot{H}_{ab})$ loops can be translated into the E–J relationship at constant values of B. To do this we have plotted $\ln \dot{H}_{ab}$ versus $\ln |M_{ab}|$ obtained from the $M_{ab}(H_{ab}, \dot{H}_{ab})$ loops at $H_{ab} = 600$ and 1000 Oe for all six values of the transverse flux. The data for $H_{ab} = 600$ Oe are shown in figure 8. Note that we have again used $|M_{ab}|$ instead of $|\Delta M_{ab}|$ for reasons previously given. All data points can be fitted by a straight line, indicating a power-law relationship between $\dot{H}_{ab}$ and M_{ab}. Since $\dot{H} \propto E$ and $M_{ab} \propto J$, the curves in figure 8 can be used to derive an E–J relationship of the form $E = AJ^n$. Clearly, the absolute magnitudes of E and J are undefined within multiplicative factors, but we are interested only in the values of n which is the physically relevant parameter. (Note that, because of the logarithmic scales, the proportionality factors between $\dot{H}$ and E and M_{ab} and J do not affect the value of n.)

Figure 9 shows the variation in the exponent n with increasing transverse flux for two values of the a–b-plane field $H_{ab} = 600$ and 1000 Oe. We find a steady decrease of n with increasing M_c^{rem}. The relatively large values of n are in keeping with the fact that n can be shown to be approximately equal to $1/C$ [22], and C as determined by us is typically much smaller than unity (see figure 5(a)). The flattening off of n at higher M_c^{rem} for $H_{ab} = 1000$ Oe is most probably due to the lower effect of the remanence when the a–b-plane field becomes large. It is well known [23] that, in the limit where flux-pinning barriers become negligible to vortex motion (flux flow), n goes towards unity. Hence a decrease in n in the presence of crossed flux again suggests a reduction in the effective pinning barriers to the motion of the a–b-plane flux.

4. Conclusions

We find in three different experiments that a remnant flux pinned along the c axis facilitates flux entry along the a–b planes. This is due to suppression of the critical currents shielding the a–b-plane flux in the presence of transverse flux. We also measure a drastic enhancement in the relaxation rate of the a–b-plane moment which, as indicated by our results, is due to a reduction in the current-dependent activation energy barriers. U_{eff} decreases linearly with increasing transverse flux, as does the critical current $J \propto M$. The measurements using the sweep-creep technique also provide evidence of reduced pinning in the CFC. The increasing creep rate C as well as the decrease in the exponent n both indicate that in the CFC the barriers to the entry of longitudinal flux are lowered.

There is a basis of similarity between our results and those obtained by LeBlanc and co-workers [8, 9], both studies being carried out on polycrystalline YBCO at $T = 77$ K. Both these results disagree, however, with the work of Park and co-workers [6, 7] on YBCO single crystals and melt-textured samples at $T = 4.2$ K.

In YBCO there exists evidence of a correlated hexagonal flux line lattice at 4.2 K, and an uncorrelated flux line lattice at 77 K [24]. We argue along the lines of [5, 11] that it is the degree of coherence of the flux lines, which enhances or inhibits the entry (or exit) of a transverse flux component. For weaker coherence of the flux lines (e.g. due to increased thermal fluctuations), the possibilities of cutting are enhanced. It has been argued that, while for rigid flux lines (i.e. at lower temperatures) the barriers to flux cutting are too high, weakly correlated flux lines, on the other hand, can locally reduce these barriers owing to their ability to twist and curve, without causing large displacements of the entire flux line lattice [5]. As obtained in [5], the barriers to flux cutting are drastically reduced by even a small amount of twist of the vortices. Hence, we believe that temperature and its effect on the morphology of flux lines may be the reason for the discrepancy between our results and those of Park and co-workers.

We explain the suppression of the critical currents (and hence the energy barriers $U_{eff}(J)$) measured in our experiments in the context of flux cutting and reconnection. It has been reported earlier [8, 9] that flux line cutting depresses the critical currents in the intergrain region of sintered YBCO samples. In our present experimental situation, the mutually perpendicular configuration of flux lines, as well as the relatively high temperatures ($T = 0.87T_c$) are favourable for flux-cutting events.

Acknowledgment

S Manzoor is grateful to the Akhter Ali Memorial Fellowship Fund for financial assistance.

References

[1] Campbell A M and Evetts J E 1972 *Adv. Phys.* **21** 199
[2] Brandt E H 1995 *Rep. Prog. Phys.* **58** 1465
[3] Clem J R 1982 *Phys. Rev.* B **26** 2463
[4] Brandt E H 1991 *Int. J. Mod. Phys.* B **5** 751
[5] Sudbo A and Brandt E H 1991 *Phys. Rev. Lett.* **67** 3176
[6] Park S J and Kouvel J S 1993 *Phys. Rev.* B **48** 13 995
[7] Park S J, Kouvel J S, Radousky H B and Lin J Z 1993 *Phys. Rev.* B **48** 13 998
[8] LeBlanc M A R, Celebi S, Wang S X and Plechácek V 1993 *Phys. Rev. Lett.* **71** 3367
[9] Celebi S and LeBlanc M A R 1994 *Phys. Rev.* B **49** 16 009
[10] Hasanain S K, Manzoor S and Amirabadizadeh A 1995 *Supercond. Sci. Technol.* **8** 519
[11] Indenbom M V, Forkl A, Ludescher B, Kronmüller H, Habermeier H-U, Leibold B, D'Anna G, Li T W, Kes P H and Menovsky A A 1994 *Physica* C **226** 325
[12] Matsushita T, Funaba S, Nagamatsu Y, Ni B, Funaki K and Yamafuji K 1989 *Japan. J. Appl. Phys.* **28** L1508
[13] Zhang L, Liu J Z, Lan M D, Klavins P and Shelton R N 1991 *Phys. Rev.* B **44** 10 190
[14] Gurevich A and Küpfer H 1993 *Phys. Rev.* B **48** 6477
[15] Anderson P W 1962 *Phys. Rev. Lett.* **9** 309
[16] Anderson P W and Kim Y B 1964 *Rev. Mod. Phys.* **36** 39
[17] Hagen C W and Griessen R 1989 *Phys. Rev. Lett.* **62** 2857
[18] Griessen R 1991 *Physica* C **172** 441
[19] Gurevich A, Küpfer H, Runtsch B, Meier-Hirmer R, Lee D and Salama K 1991 *Phys. Rev.* B **44** 12 090
[20] Sun Y R, Thompson J R, Christen D K, Ossandon J G, Chen Y J and Goyal K 1992 *Phys. Rev.* B **46** 8480
[21] Delin K A, Orlando T P, Mc Niff E J, Foner S, Van Dover R B, Schneemeyer L F and Waszcak J V 1992 *Phys. Rev.* B **46** 11 092

[22] Caplin A D, Cohen L F, Perkins G K and Zhukov A A 1994 *Semicond. Sci. Technol.* **7** 412
[23] Blatter G, Feigel'man M V, Geshkenbein V B, Larkin A I and Vinokur V M 1994 *Rev. Mod. Phys.* **66** 1125
[24] Gammel P L, Schneemeyer L F, Waszczak J V and Bishop D J 1988 *Phys. Rev. Lett.* **61** 1666